OPEN ACCESS
JOURNAL OF ADVANCED DIELECTRICS
Vol. 11, No. 5 (2021) 2160018 (7 pages)
© The Author(s)
DOI: 10.1142/S2010135X21600183

Structure and dielectric properties of solid solutions $Bi_{7-2x}Nd_{2x}Ti_4NbO_{21}$ (x = 0.0, 0.2, 0.4, 0.6, 0.8, 1.0)

S. V. Zubkov

Research Institute of Physics
Southern Federal University
pr. Stachki 194, Rostov-on Don
344090 Russia

Department "International"
Don State Technical University
1, pr.Gagarina, Rostov-on-Don
344003, Russia

svzubkov61@mail.ru

Received 18 April 2021; Revised 5 June 2021; Accepted 8 June 2021; Published 18 August 2021

The electrophysical and structural characteristics of bismuth titanate oxides of a number of phases of solid solutions of the Aurivillius phases $Bi_{7-2x}Nd_{2x}Ti_4NbO_{21}$ (x = 0.0, 0.2, 0.4, 0.6, 0.8, 1.0) having a layered structure of the perovskite type have been investigated. According to the XRD data, all studied compounds are single-phase and have a mixed-layer structure of Aurivillius phases (m = 2.5) with a rhombic crystal lattice (space group *I2cm*, Z = 2). A relationship has been established between changes in the chemical composition of solid solutions and orthorhombic and tetragonal distortions of perovskite-like layers. The temperature dependences of the relative permittivity $\varepsilon/\varepsilon_0$(T) are measured. It was found that the change in the phase transition temperature — Curie temperature T_C synthesized Aurivillius phases $Bi_{7-x}Nd_{2x}Ti_4NbO_{21}$ (x = 0.0, 0.2, 0.4, 0.6, 0.8, 1.0) has a close to linear dependence on the change in the parameter x. The activation energies of charge carriers in different temperature ranges were calculated. It was found that three clearly defined temperature ranges with different activation energies can be distinguished, which is associated with the different nature of charge carriers in the studied solid solutions of the perovskite type. The effect of substitution of Nd^{3+} ions for Bi^{3+} ions is investigated.

Keywords: Aurivillius phases; $Bi_{7-2x}Nd_{2x}Ti_4NbO_{21}$; Curie temperature ($T_C$); tolerance factor.

1. Introduction

One of the remarkable types of compounds in the series of Aurivillius Phases (APs)[1–3] is mixed-layer compounds. The mixed-layer compounds of the family of bismuth-containing layered compounds of the perovskite type have a chemical composition that is described by the formula $A_{m-1}Bi_2B_mO_{3m+3}$, common for the entire family of APs. The crystal structure of mixed-layer compounds of APs consists of alternating layers of $[Bi_2O_2]^{2+}$, separated by an even and odd number layers (m and m+1) $[A_{m-1}BmO_{3m+1}]^{2-}$, where the position A in the dodecahedra is occupied by ions with radii greater than 1 Å by the lone electron pair s^2 (Bi^{3+}, Sr^{2+}, Y^{3+}, Ln^{3+} (lanthanides)) have, while the B-positions inside the oxygen octahedra are occupied by ions with a radius less than 0.7 Å and having in the ground state the shell of the s^2p^6 noble gas atom (Ti^{4+}, Nb^{5+}, Ta^{5+}, W^{6+}, Ga^{3+}, etc.). Interest in mixed-layer compounds, on the one hand, is due to the fact that they have two phase transitions. On the other hand, it is caused by practical problems — possible applications in the development and production of high-temperature piezoelectric sensors operating in extreme conditions, as elements of nonvolatile ferroelectric random access memory (FeRAM),[4,5] as multifunctional materials exhibiting both ferroelectric and magnetic properties (multiferroics).[6,7] The possibility of a significant variation in the composition due to the substitution of A and B ions with a simultaneous change in the crystal structure due to an increase in the number of layers m = 1–6 makes it possible to obtain a large number of Aps.[8,9] The main task of the study is to establish relationships between the chemical composition, crystal structure and dielectric properties of new APs. As can be seen from our previous works, the introduction of changes in the composition of the APs due to the addition of a certain amount of donor impurities, such as W^{6+},V^{5+}, Re^{7+}, etc., leads to a decrease in the number of oxygen vacancies and a decrease in the leakage current.[10] Doping with APs allows an increase in the dielectric constant, as well as a controlled change in the Curie temperature T_c, in a possible temperature range. When doped with the $SrBi_2(W_xTa_{1-x})_2O_9$ (x = 0.0, 0.2) composition, an increase in the residual polarization of tungsten SBT ceramics with an increase tungsten up to $x \le 0.075$.[11–16]

This is an Open Access article published by World Scientific Publishing Company. It is distributed under the terms of the Creative Commons Attribution 4.0 (CC BY) License which permits use, distribution and reproduction in any medium, provided the original work is properly cited.

The $Bi_7Ti_4NbO_{21}$ compound belongs to mixed-layer APs with $m = 2.5$, in which layers with an even number $m = 2$ of the initial APs (Bi_3TiNbO_9) and an odd number $m = 3$ of the initial APs ($Bi_4Ti_3O_{12}$) alternate regularly.

In this work, we investigated the relationship between the chemical composition, structural changes and electrophysical properties of a mixed-layer compound of a series of solid solutions APs $Bi_{7-2x}Nd_{2x}Ti_4NbO_{21}$ ($x = 0.0, 0.2, 0.4, 0.6, 0.8, 1.0$). Structural studies were carried out using X-ray diffraction patterns and the temperature dependences of the dielectric characteristics of new APs from the series: $Bi_7Ti_4NbO_{21}$, $Bi_{6.6}Nd_{0.4}Ti_4NbO_{21}$, $Bi_{6.2}Nd_{0.8}Ti_4NbO_{21}$, $Bi_{5.8}Nd_{1.2}Ti_4NbO_{21}$, $Bi_{5.4}Nd_{1.6}Ti_4NbO_{21}$, $Bi_{5.0}Nd_{2.0}Ti_4NbO_{21}$.

2. Experimental Methods

The polycrystalline samples APs were obtained by solid-phase reaction. To obtain the samples, the corresponding oxides Bi_2O_3, Nd_2O_3, TiO_2, Nb_2O_5 of high purity were used. A mixture of oxides of stoichiometric composition of the starting compounds was weighed, thoroughly crushed and mixed with the addition of ethyl alcohol, pressed and calcined at a temperature of 890 °C for 2 h. Then the samples were re-crushed to a uniform consistency, compressed into tablets 10 mm in diameter and 1.0–1.5 mm, followed by the final synthesis of APs at a temperature of 1120 °C (for 4 h). X-ray diffraction patterns were obtained on a DRON-3M diffractometer with a 1.5BSV29Cu X-ray tube. With the help of a Ni-filter, the radiation of Cu K_{α_1,α_2} was separated from the general spectrum. The measurement range of the diffraction patterns of the angles 2θ was in the range from 10° to 65°, the scanning step was 0.04°, the exposure was 10 s at a point. The PCW 2.4 program[17] was used to: refine the unit cell parameters, determine the position of lines, analyze the profiles of diffraction patterns and index them (*hkl*). To measure the change in the temperature dependence of the dielectric constant and electrical conductivity, electrodes were applied using an Ag–Pd paste on the preliminarily ground and degreased surfaces of APs samples in the form of disks 10 mm in diameter and about 1–1.5 mm thick. The Ag–Pd paste was burned in at a temperature of 820 °C (1 h). The dependences of dielectric characteristics on temperature and frequency were measured using an E7-20 immittance meter in the frequency range from 100 kHz to 1 MHz and in the temperature range from room temperature to temperatures exceeding the Curie temperature T_c by 30 °C.

3. Results and Discussion

Diffraction patterns of powders of all studied solid solutions $Bi_{7-2x}Nd_{2x}Ti_4NbO_{21}$ ($x = 0.0, 0.2, 0.4, 0.6, 0.8, 1.0$) corresponded to single-phase APs with $m = 2.5$ and did not contain additional reflections. Figure 1 shows the powder diffraction pattern of the $Bi_{7-2x}Nd_{2x}Ti_4NbO_{21}$ sample ($x = 0.2, 0.4, 0.6, 0.8, 1.0$). It was found that all synthesized APs under study crystallized into an orthorhombic structure with a unit cell space group *I2cm* (46).

From the X-ray diffraction data, the unit cell parameters and unit cell volume were determined. Table 1 shows the parameters of the orthorhombic δb and tetragonal $\delta c'$ deformation; average tetragonal period a_t, tolerance factor t; and the average thickness of a single perovskite layer c'. The obtained unit cell parameters for the studied APs $Bi_{7-2x}Nd_{2x}Ti_4NbO_{21}$ ($x = 0$) sample are close to those determined earlier: $a = 5.4469$ (4) Å, $b = 5.4121$ (4) Å, $c = 58.0429$ (47) Å (Ref. 18); $a = 5.45$ Å, $b = 5.42$ Å, $c = 58.1$ Å (Ref. 19); $a = 5.44$ Å, $b = 5.40$ Å, $c = 58.1$ Å (Ref. 20); $a = 5.442$ (1) Å, $b = 5.404$ (1) Å, $c = 57.990$ (12) Å (single

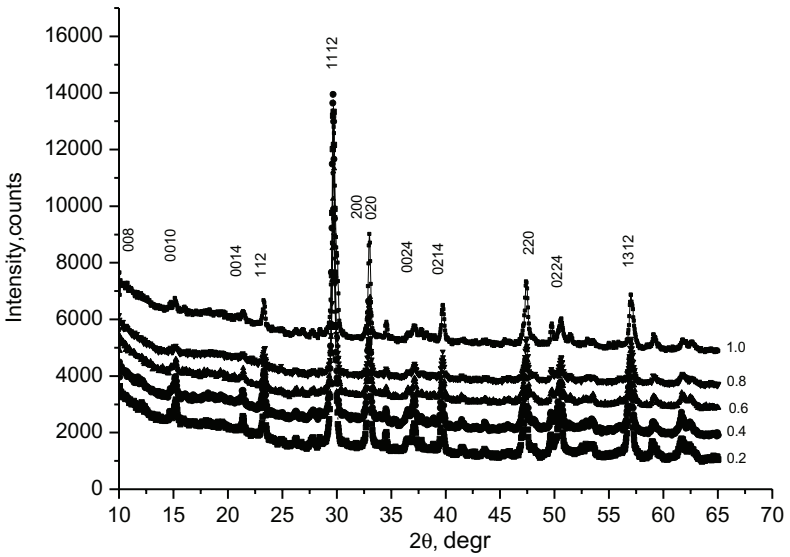

Fig. 1. X-ray powder diffraction patterns of $Bi_{7-2x}Nd_{2x}Ti_4NbO_{21}$ ($x = 0.2, 0.4, 0.6, 0.8, 1.0$) (space group *I2cm*).

Table 1. Unit cell parameters *a*,*b*,*c*,*V*, and value of tolerance-factor *t* of APs $Bi_{7-2x}Nd_{2x}Ti_4NbO_{21}$ (x = 0.0, 0.2, 0.4, 0.6, 0.8, 1.0); parameters of the orthorombic δb and tetragonal $\delta c'$ strains; average tetragonal period a_t, and average thickness of single perovskite layer c'.'

Compounds	*a*, Å	*b*, Å	*c*, Å	*V*, Å^3	*t*	a_t, Å	δb,%	$\delta c'$, %	c', Å
$Bi_7Ti_4NbO_{21}$	5.444 (9)	5.4114	58.01	1708.95	0.948	3.834	0.698	−1.428	3.781
$Bi_{6.6}Nd_{0.4}Ti_4NbO_{21}$	5.4623	5.4381	58.09	1725.536	0.958	3.848	0.714	−1.559	3.788
$Bi_{6.2}Nd_{0.8}Ti_4NbO_{21}$	5.4564	5.4179	58.09	1717.27	0.957	3.844	0.696	−1.482	3.787
$Bi_{5.8}Nd_{1.2}Ti_4NbO_{21}$	5.4595	5.4187	58.09	1718.49	0.9558	3,843	0.766	−1.456	3.788
$Bi_{5.4}Nd_{1.6}Ti_4NbO_{21}$	5.4567	5.4149	58.07	1715.91	0.9546	3.846	0.747	−1.501	3.788
$Bi_{5.0}Nd_{2.0}Ti_4NbO_{21}$	5.4664	5.4517	58.09	1719.464	0.9534	3.861	0.268	−1.865	3.788

crystal).[21] The unit cell structure of APs $Bi_7Ti_4NbO_{21}$ can be described as the alternation of the initial phases with $m = 2$ (Bi_3TiNbO_9) and $m = 3$ ($Bi_4Ti_3O_{12}$). It was previously found that this compound has a higher residual polarization compared to the two initial APs along the *c*-axis, where the $BiTiNbO_7$ building blocks contain an equal amount of Ti^{4+} and Nb^{5+} ions in the perovskite layer and the Bi_2O_2 layers and the perovskite-like $Bi_2Ti_3O_{10}$ layer are separated with $m = 3$ — blocks without niobium ions. These blocks $BiTiNbO_7$ with $m = 2$ and $Bi_2Ti_3O_{10}$ with $m = 3$ are displaced relative to the [100] direction by 1/2 cell. Blocks of octahedra in perovskite-like layers have distortions along the *c*-axis (compression or tension), as well as tilt around the *a*-axis and rotation around the *c*-axis.[22,23] Figure 2 shows the dependence of the unit cell parameters on the parameter *x*. As can be seen from Fig. 2, the change in the unit cell volume in this series does not exceed 2%. It was found that the change in the unit cell parameters of the APs $Bi_{7-2x}Nd_{2x}Ti_4NbO_{21}$ is related, among other things, to the difference in radii in the ions in position A having dodecahedral coordination in the perovskite-like layer, where position A is occupied by Bi^{3+} ions (R^{3+}_{Bi} = 1.33 Å and are replaced by Nd^{3+} ions with a much smaller radius ($R_{Nd}{}^{3+}$ = 1.27 Å). It should be noted that the observed decrease in the unit cell volume at x = 0.2–0.4 is associated only with a change in the unit cell parameters *b* and *a*. The unit cell volume at x = 1.0 increases again. In this work, the tolerance factor *t* was calculated using the Goldschmidt formula (1):

$$t = (R_A + R_O)/\sqrt{2}\,(R_B + R_O), \quad (1)$$

where R_A and R_B are the radii of cations in positions A and B, respectively; R_O is the ionic radius of oxygen.[24] The calculation of the tolerance coefficient *t* was carried out taking into account the ionic radii of the Shannon data with the corresponding coordination numbers (CN) (O^{2-} (CN = 6) R_O = 1.40 Å, Nd^{3+} (CN = 6) R_{Nd} = 1.27 Å, Nb^{5+} (CN = 6) R_{Nb} = 0.64 Å, Ti^{4+} (CN = 6) R_{Ti} = 0.605 Å) Shannon[25] did not provide the ionic radius of Bi^{3+} for coordination with CN = 12. Therefore, its value was determined. From the ionic radius with CN = 8 (R^{3+}_{Bi} = 1.17 Å), multiplied by the approximation factor of 1.136, then for Bi^{3+} (CN = 12) we got R^{3+}_{Bi} = 1.33 Å. As you can see from Table 1, all the tolerance factor *t* for synthesized lie in a rather narrow range of 0.95. This range is in the center of the region of maximum stability of cubic structures, which is characterized by the values $0.9 \le t \le 1.0$. The obtained values of the orthorhombic deformation $\delta b = (b - a)/a$ – rhombic deformation, $\delta c' = (c' - a_t)/a_t$ is the deviation of the cell from the cubic shape, that is, lengthening or shortening along the *c*-axis, (where $a_t = (a_0 + b_0)/a$ is the deviation of the cell from the cubic shape, that is, lengthening or shortening along the *c*-axis, $c' = 3c\ /(8 + 6m)$ the average thickness *c* of one perovskite layer) (Table 1).[26]

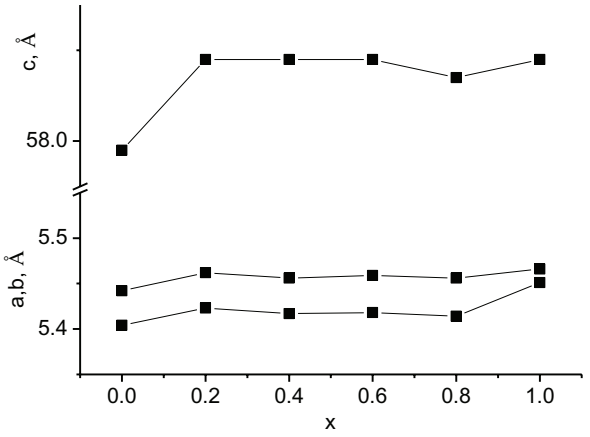

Fig. 2. Dependences of the unit cell parameters *a*, *b*, *c* in solid solutions.

It can be seen from Table 1 that, as the parameter *x* changes into range of x = 0–0.4, the orthorhombic distortion of the pseudoperovskite unit cell significantly decreases as compared to the undoped $Bi_7Ti_4NbO_{21}$. For the entire series of Nd^{3+}, the tolerance factor *t* increases due to the decrease in the concentration of Nb^{5+} ions with the largest ionic radius, whereas the average tetragonal period a_t and the average thickness of the single perovskite layer systematically decrease.

In addition to the results of structural studies, the temperature dependences of the relative permittivity $\varepsilon/\varepsilon_o(T)$ and the

values of the tangent of the angle of dielectric losses at various frequencies of 100–1000 kHz were obtained. The activation energies E_a of charge carriers are calculated for different temperature ranges. Figure 3 shows the temperature dependences of the relative permittivity $\varepsilon/\varepsilon_o(T)$ and of the tangent of the angle of dielectric losses for $Bi_{7-2x}Nd_{2x}Ti_4NbO_{21}$ (x = 0.0–1.0) at a frequency of 100 kHz–1 MHz. All $\varepsilon/\varepsilon_o(T)$ dependences have two features at temperatures T_1 and T_2, for which the corresponding values of the dielectric constant are given in Table 2.

The first peak on the $\varepsilon/\varepsilon_o(T)$ dependence at temperature T_2 corresponds to the phase transition from the polar to the polar

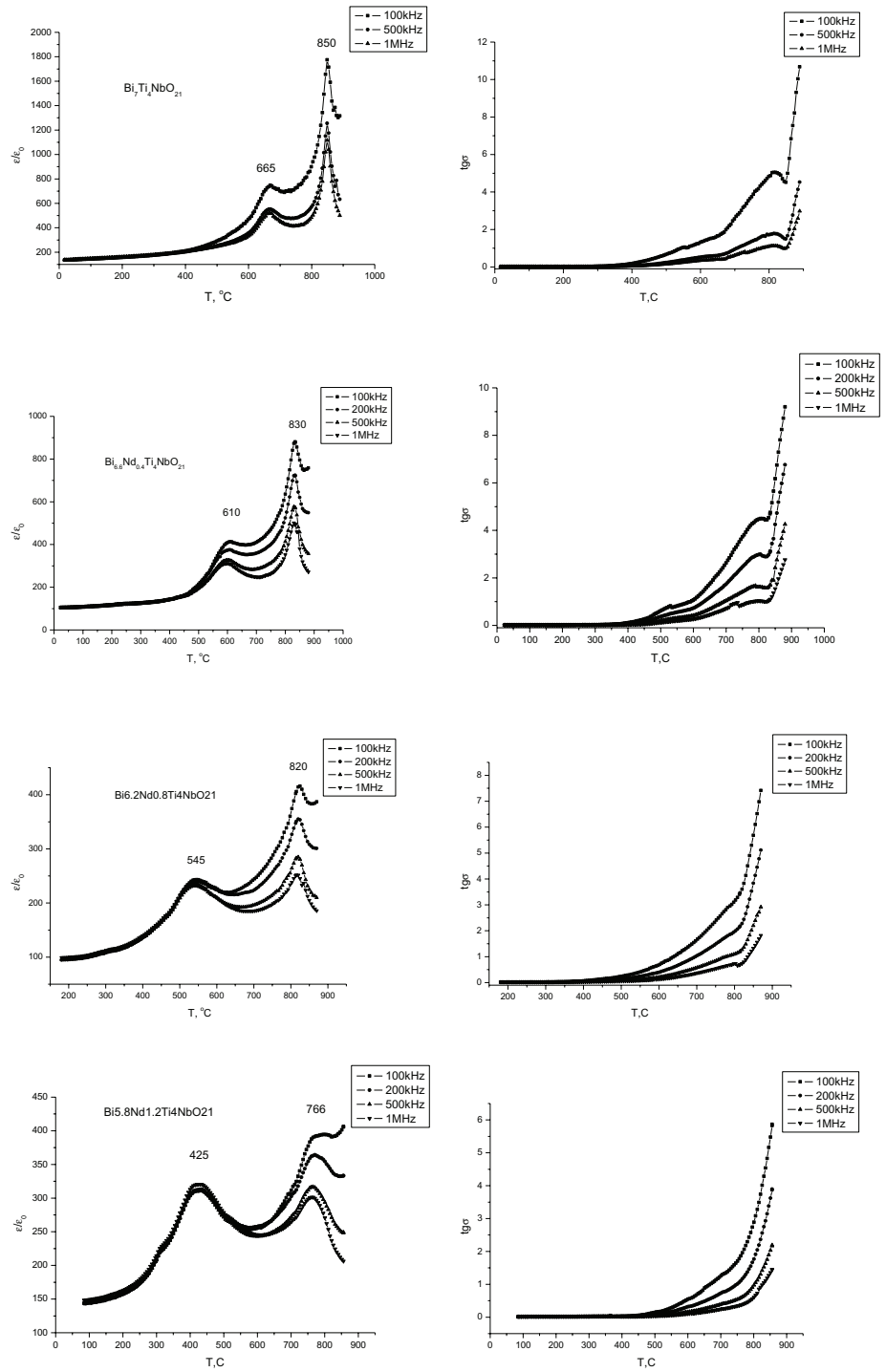

Fig. 3. Temperature dependences of the relative permittivity $\varepsilon/\varepsilon_o$(T) (left panels) and loss tgσ (right panels) of $Bi_{7-2x}Nd_{2x}Ti_4NbO_{21}$ (x = 0.0, 0.2, 0.4, 0.6, 0.8, 1.0) measures at of 100 kHz–1MHz.

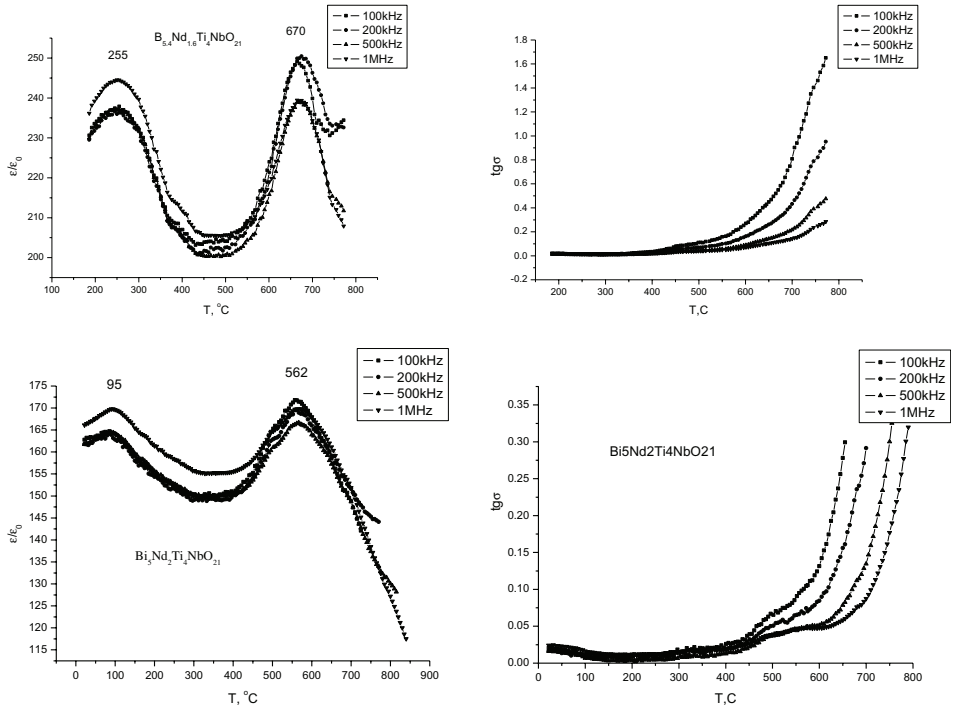

Fig. 3. (*Continued*)

Table 2. Dielectric characteristics of $Bi_{7-2x}Nd_{2x}Ti_4NbO_{21}$ (x = 0.0, 0.2, 0.4, 0.6, 0.8, 1.0).

Compounds	t	$\varepsilon/\varepsilon_0(T_1/T_2)$ (100 kHz)	T_1, °C	T_2, °C	$E_1/E_2/E_3$, eV
$Bi_7Ti_4NbO_{21}$	0.948	1800/900	850	665	0.9/0.3/0.02
$Bi_{6.6}Nd_{0.4}Ti_4NbO_{21}$	0.958	900/500	830	610	0.81/0.24/0.01
$Bi_{6.2}Nd_{0.8}Ti_4NbO_{21}$	0.957	400/250	820	545	1.73/0.23/0.11
$Bi_{5.8}Nd_{1.2}Ti_4NbO_{21}$	0.9558	400/325	766	425	1.16/0.55
$Bi_{5.4}Nd_{1.6}Ti_4NbO_{21}$	0.9546	250/245	670	255	0.9/0.48/0.03
$Bi_5Nd_2Ti_4NbO_{21}$	0.9534	172/172	562	95	0.8/0.33/0.06

phase (ferroelectric–ferroelectric), this transition in the temperature range from T_1 to T_2 is accompanied by the removal of distortions for the $Bi_2Ti_3O_{10}$ perovskite block with $m = 3$, while in the $BiTiNbO_7$ perovskite block with $m = 2$, the distortions of the octahedral layers are retained.

At temperatures above T_1, distortions are removed in both blocks of the perovskite type, and the Nd^{3+} symmetry is close to *I4*/mmm. Thus, the temperature T_1 corresponds to the transition from the polar to the nonpolar phase (paraelectric–ferroelectric phase), this is the Curie temperature T_C. Replacement of Bi^{3+} ions in cuboctahedra by ions with a smaller ionic radius usually leads to significant changes in the dielectric characteristics of these compounds. Accordingly, it should be expected that there is a dependence of the temperature T_1 on the tolerance coefficient t due to changes in the average radii of the A ions. Figure 4 shows the dependences of the temperatures T_1 and T_2 on the parameters x

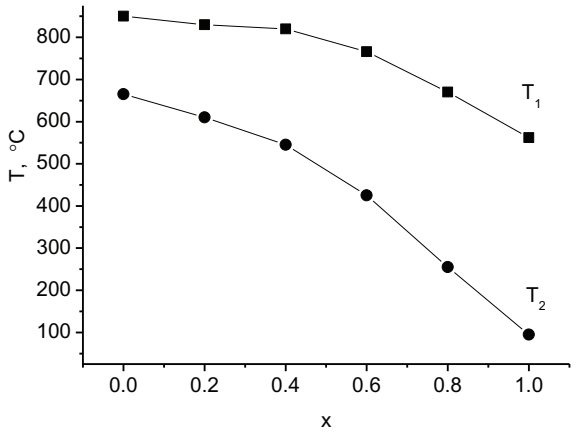

Fig. 4. Dependences of the temperature T_C of the synthesized $Bi_{7-2x}Nd_{2x}Ti_4NbO_{21}$ (x = 0.0, 0.2, 0.4, 0.6, 0.8, 1.0) on the parameter x.

and t for $Bi_{7-2x}Nd_{2x}Ti_4NbO_{21}$, which turned out to be unexpected for this type of substitution. It should be noted that with an increase in neodymium concentration, the decrease in temperature T_2 is much more pronounced (it decreases by almost 500 °C) compared to $T_1(x)$ (which decreases by only about 270 °C). A possible explanation for the difference in the dependences $T_1(x)$ and $T_2(x)$ may be the assumption that the substitution of Bi^{3+} ions in cuboctadra by Nd^{3+} ions occurs mainly not in most distorted perovskite layers of $BiTiNbO_7$ with $m = 2$ and, but to a greater extent, in a more symmetric compound $Bi_2Ti_3O_{10}$ with $m = 3$. The maxima on the temperature dependence of the dielectric constant $\varepsilon(T)$ do not show any dependence on the composition of $Bi_{7-2x}Nd_{2x}Ti_4\ NbO_{21}$ (Table 2). Since the dielectric constant ε depends on many factors (composition, grain size, porosity, concentration of vacancies, etc.), the combination of all these factors neutralizes this dependence. The obtained values of the activation energy E_a of charge carriers in $Bi_{7-2x}Nd_{2x}Ti_4NbO_{21}$ are presented in Table 2. The activation energy E_a was determined from the Arrhenius equation:

$$\sigma = A/T \exp(-E_a/kT), \quad (2)$$

where σ is the electrical conductivity, k is the Boltzmann's constant, and A is the constant. A typical dependence of $\ln\sigma$ on 10,000/kT (at a frequency of 100 kHz), which was used to determine the activation energies E_a, is shown in Fig. 5 for the AP $Bi_{5.8}Nd_{1.2}Ti_4NbO_{21}$. Figure 5 clearly shows that there are three temperature regions in which the activation energies E_a have significantly different values. For two high temperature regions, characterized by high activation energies of charge carriers, the values E_a (1) > E_a (2) differ from each other by almost two times, and the boundary of the change in the activation energy is close to the phase transition temperature T_1. It should be noted that the values of E_a corresponding to the electrical conductivity in a wide temperature range from 300 °C to T_2 systematically decrease with increasing doping with Nd^{3+} ions for all members of the $Bi_{7-2x}Nd_{2x}Ti_4NbO_{21}$ series, while in the high-temperature region above T_1 for E_a such dependence is not observed. It is known that, in a wide temperature range, the determining factor is ionic conductivity, which occurs by the mechanism of oxygen ions jumping into existing vacancies in the crystal lattice.

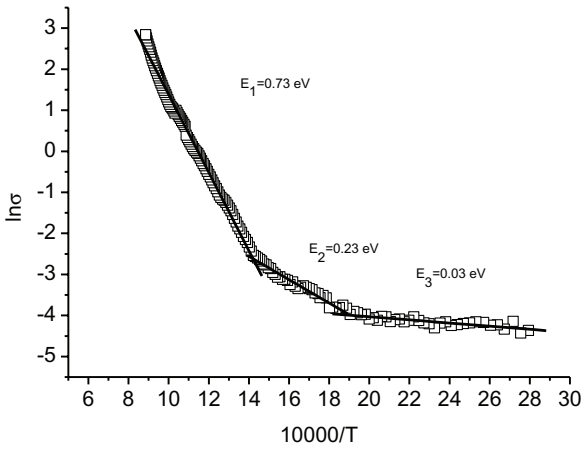

Fig. 5. Dependence of $\ln\sigma$ on 10,000/T for the $Bi_{5.8}Nd_{1.2}Ti_4NbO_{21}$ sample.

This intrinsic conductivity is characterized by relatively high charge carrier activation energies of approximately 1 eV. The doping of Nd^{3+} by different cations can lead to a change in their conductivity, both toward an increase with the formation of additional oxygen vacancies and toward a decrease, when these vacancies are bound with doped metal ions. The systematic decrease in the activation energy in the series of $Bi_{7-2x}Nd_{2x}Ti_4NbO_{21}$ with an increase in the concentration of Nd^{3+} ions, which leads to an increase in the electrical conductivity, indicates the first mechanism of change in the electrical conductivity of this Nd^{3+}. The obtained values for the studied series of $Bi_{7-2x}Nd_{2x}Ti_4NbO_{21}$ are close to the characteristic values of the activation energy (approximately 0.5–1.0 eV) for oxygen vacancies in the Nd^{3+}. The nature of the conductivity in APs at temperatures above T_2 with higher values of E_a (1) > 1.5 eV requires further investigation. In the low-temperature range, the electrical conductivity is predominantly determined by impurity defects with very low activation energies of the order of a few hundredths of an electron-volt.

4. Conclusion

(1) Series of layered bismuth perovskite oxides $Bi_7Ti_4NbO_{21}$, $Bi_{6.6}Nd_{0.4}Ti_4NbO_{21}$,$Bi_{6.2}Nd_{0.8}Ti_4NbO_{21}$,$Bi_{5.8}Nd_{1.2}Ti_4NbO_{21}$, $Bi_{5.4}Nd_{1.6}Ti_4NbO_{21}$, $Bi_{5.0}Nd_2Ti_4NbO_{21}$ were synthesized by the solid-state method.

(2) The X-ray structural studies carried out in our work showed that all the compounds obtained have the APs structure ($m = 2.5$) with an orthorhombic crystal lattice (space group $I2cm$, $Z = 2$).

(3) An analysis of the details of the structure of the APs showed that an increase in the concentration x of neodymium x from 0.2 to 1.0 and a partial replacement of bismuth ions with niodimium ions lead to a decrease in the tangent of the dielectric loss angle and a decrease in $\varepsilon/\varepsilon_o(T)$. The temperature dependences $\varepsilon/\varepsilon_o(T)$ in $Bi_{7-2x}Nd_{2x}Ti_4NbO_{21}$ compounds (x = 0.0, 0.2, 0.4, 0.6, 0.8, 1.0) exhibit two anomalies:

   (a) the low-temperature anomaly corresponds to a ferroelectric phase transition;

   (b) the high-temperature anomaly is associated with the Curie temperature T_c corresponding to the ferroelectric phase of the paraelectric transition.

(4) Ligation with neodymium ions $Bi_{7-2x}Nd_{2x}Ti_4NbO_{21}$ results in:

   (a) to a significant shift of low-temperature peaks towards a decrease (500 °C).

   (b) and less significant shift of T_c towards decrease (150 °C).

Acknowledgments

The study was financially supported by the Ministry of Science and Higher Education of the Russian Federation [State task in the field of scientific activity, scientific project No. 0852-2020-0032 (BAS0110/20-3-08IF)].

References

[1]B. Aurivillius, Mixed bismuth oxides with layer lattices: I. Structure type of $CaBi_2B_2O_9$, *Arkiv. Kemi*. **1**, 463 (1949).

[2]B. Aurivillius, Mixed bismuth oxides with layer lattices: II. Structure type of $Bi_4Ti_3O_{12}$, *Arkiv. Kemi*. **58**, 499 (1949).

[3]B. Aurivillius, Mixed bismuth oxides with layer lattices: III. Structure type of $BaBi_4Ti_4O_{15}$, *Arkiv. Kemi*. **37**, 512 (1950).

[4]B. H. Park, B. S. Kang, S. D. Bu, T. W. Noh, J. Lee and W. Jo, Lantanum-substituted bismuth titanate for use in non-voatile memories, *Nature* **401**, 682 (1999).

[5]A. P. de Araujo, J. D. Cuchiaro, L. D. Mcmillan, M. C. Scott and J. F. Scott, Electromechanical properties of A-site (LiCe) – modified sodium bismuth titanate ($Na_{0.5}Bi_{4.5}Ti_4O_{15}$) piezoelectric ceramics at elevated temperature, *Nature* **374**, 627 (1995). https://doi.org/10.1063/1.3117219.

[6]X. Chen, J. Xiao, Y. Xue, X. Zeng, F. Yang and P. Su, Room temperature multiferroic properties of Ni-doped Aurivillius phase $Bi_3Ti_3FeO_{15}$, *Ceram. Int*. **40**, 2635 (2014). https://doi.org/10.1016/j.ceramint.2013.10.063.

[7]V. G. Vlasenko, V. A. Shuvaeva, S. I. Levchenkov, Ya. V. Zubavichus and S. V. Zubkov, Structural, electric al and magnetic characterization of a new Aurivillius $Bi_{5-x}Th_xFe^+{}_xTi_{3-x}O_{15}$ ($x = 1/3$), *J. Alloys Compd*. **610**, 184 (2014). https://doi.org/10.1016/j.jallcom.2014.04.045.

[8]S. V. Zubkov, V. G. Vlasenko, V. A. Shuvaeva and S. I. Shevtsova, Structure and dielectric properties of solid solutions $Bi_7Ti_{4+x}W_xTa_{1-2x}O_{21}$ (x = 0–0.5), *J. Phys. Solid State* **58**(1), 44 (2016). https://doi.org/10.1134/S1063783416010352.

[9]T. Wang, J. Hu, H. Yang, L. Jin, X. Wei, C. Li, F. Yan and Y. Lin, Dielectric relaxation and Maxwell-Wagner interface polarization in Nb_2O_5 doped $0.65BiFeO_3$–0.35 BaTi O_3 ceramics, *J. Appl. Phys*. **121**, 084103 (2017). https://doi.org/10.1063/1.4977107.

[10]S. V. Zubkov and V. G. Vlasenko, Crystal structure and dielectric properties of layered perovskite-like solid solutions $Bi_{3-x}Y_xTiNbO_9$ ($x = 0, 0.1, 0.2, 0.3$) with high Curie temperature, *J. Phys. Solid State* **59**(12), 2325 (2017). https://doi.org/ 10.1134/S1063783417120332.

[11]I. Coondoo, S. K. Agarwal and A. K. Jha, Ferroelectric and piezoelectric properties of tungsten substituted $SrBi_2Ta_2O_9$ ferroelectric ceramics, *Mater. Res. Bull*. **44**, 1288 (2009), https://doi.org/10.1016/j.materresbull.2009.01.001.

[12]I. Coondoo, N. Panwar and A. K. Jha, Effect of sintering temperature on the structural, dielectric and ferroelectric properties of tungsten substituted SBT ceramics, *Physica B: Cond. Mat.* **406**, 374 (2011), https://doi.org/10.1016/j.physb.2010.10.074.

[13]J. K. Kim, T. K. Song, S. S. Kim and J. Kim, Ferroelectric properties of tungsten-doped bismuth titanate thin film prepared by sol–gel route *Mater. Lett*. **57**, 964 (2002), https://doi.org/10.1016/S0167-577X(02)00906-0.

[14]W. T. Lin, T. W. Chiu, H. H. Yu, J. L. Lin and S. Lin, Effects of W doping and annealing parameters on the ferroelectricity and fatigue properties of sputtered $Bi_{3.25}La_{0.75}Ti_3O_{12}Bi_{3.25}La_{0.75}Ti_3O_{12}$ films, *J. Vac. Sci. Technol*., *A* **21**, 787 (2003), https://doi.org/10.1116/1.1570840.

[15]Y. Wu, S. J. Limmer, T. P. Chou, Influence of tungsten doping on dielectric properties of strontium bismuth niobate ferroelectric ceramics, *J. Mater. Sci. Lett*. **21**, 947 (2002), https://doi.org/10.1023/A:1016077724427.

[16]C. Long, H. Fan, M. Li and Q. Li, Effect of lanthanum and tungsten co-substitution on the structure and properties of new Aurivillius oxides $Na_{0.5}La_{0.5}Bi_2Nb_{2-x}W_xO_9$, *Cryst. Eng. Commun.* **14**, 7201 (2012), https://doi.org/10.1039/c2ce25718a.

[17]W. Kraus and G. Nolze, *PowderCell for Windows. Version 2.3* (Federal Institute for Materials Research and Testing, Berlin, 1999).

[18]A. Yokoi and H. Ogawa, Crystal structure and ferroelectric properties of mixed bismuth layers structure $Bi_7Ti_{4+x/2}Nb_{1-x}W_{x/2}O_{21}$ ceramics. *Mater. Sci. Eng*. *B* **129**, 80 (2006). https://doi.org/10.1016/j.mseb.2005.12.023.

[19]S. Horiuchi, T. Kikuchi and M. Goto, Structure determination of a mixed-layers bismuth titanateniobate, $Bi_7Ti_4NbO_{21}$, by super–high-resolution electron microscopy, *Acta Crystallogr., Sect. A: Cryst. Phys., Diffr., Theor. Gen. Crystallogr*. **33**, 701 (1977). https://doi.org/10.11077/S0567739477001806.

[20]P. Duran, F. Capel, C. Moure, M. Villegas, J. F. Fernandez, J. Tartaj and A. C. Caballero, Processing and dielectric properties of the mixed-layers bismuth titanateniobate $Bi_7Ti_4NbO_{21}$ by the metal-organic precursor synthesis method, *Eur. Ceram. Soc*. **21**, 1 (2001). https://doi.org/10.016/S0955-2219(00)00161-8.

[21]D. Mercurio, G. Trolliard, T. Hansen and J. P. Mercurio, Crystal structure of the ferroelectrics mixed Aurivillius phase $Bi_7Ti_4NbO_{21}$ *Int. J. Inorg. Mater*. **2**(5), 397 (2000). https://doi.org/10.016/S1466-6049(00)00090-8.

[22]F. Chu, D. Damjanovic, O. Steiner and N. Setter, Piezoelectricity and phase transitions of mixed-layer bismuth titanate niobate $Bi_7Ti_4NbO_{21}$, *J. Am. Ceram. Soc*. **78**, 3142 (1995). https://doi.org/10.1111/j.1151-2916.1995.tb09099.x.

[23]Z. G. Yi, Y. Wang, Y. X. Li and Q. R. Yin, Ferroelectricity in intergrowth Bi_3TiNbO_9–$Bi_4Ti_3O_{12}$ ceramics, *J. Appl. Phys*. **99**, 114101 (2006), doi:10.1063/1.2199751.

[24]V. M. Goldschmidt, *Geochemische Verteilungsgesetze der Elemente* (Norske, Oslo, 1927).

[25] R. D. Shannon, *Acta Crystallogr., Sect. A: Cryst. Phys., Diffr., Theor. Gen. Crystallogr*. **32**, 75 (1976). https://doi.org/10.1107/S0567739476001551.

[26]A. Isupov, Properties of perovskite-like laminated ferroelectric compounds of $A_{m-1}Bi_2M_mO_{3m+3}$ type, *J. Neorg. Khim*. **39**, 731 (1994).